ChemComm

Accepted Manuscript

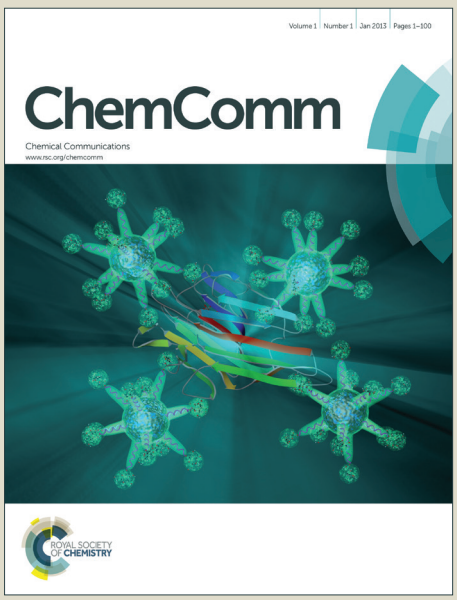

ROYAL SOCIETY OF CHEMISTRY

www.rsc.org/chemcomm

ChemComm

RSCPublishing

COMMUNICATION

A Quartz Crystal Microbalance Method to Study the Terminal Functionalization of Glycosaminoglycans

Cite this: DOI: 10.1039/x0xx00000x

Dhruv Thakar,[a,b] Elisa Migliorini,[a,b] Liliane Coche-Guerente,[a,b] Rabia Sadir,[c,d,e] Hugues Lortat-Jacob,[c,d,e] Didier Boturyn,[a,b] Olivier Renaudet,[a,b] Pierre Labbe[a,b] and Ralf P. Richter*[a,b,f,g]

Received,
Accepted

DOI: 10.1039/x0xx00000x

www.rsc.org/

We demonstrate quartz crystal microbalance as a novel method to quantify reaction yields and stability of the terminal conjugation of chemically complex molecules. Oxime ligation is identified as a facile, broadly applicable method for the reducing-end conjugation of glycosaminoglycans that overcomes the limited stability and yield of popular hydrazone ligation.

Linear polysaccharides known as glycosaminoglycans (GAGs) are ubiquitous cell surface and extracellular matrix components and fulfill crucial biological functions. Advanced screening applications (e.g. glycan microarrays[1, 2]), functional molecular and cellular assays,[3] as well as biosensors and biomaterials[4] require the attachment of GAGs to surfaces or other scaffolds (e.g. with a biotin that can be anchored to biotin-binding proteins). In this regard, site-specific conjugation through the reducing end is desirable, as it effectively mimics the cell surface presentation of GAG motives and avoids alteration of GAG-protein interactions by chemical modifications along the GAG chain, or by surface-imposed conformational or spatial constraints.[5]

An important but still underestimated challenge with the conjugation of GAG-derived oligosaccharides, and in particular polymeric GAGs, is the characterization of the reaction products. The often low isolation yields from natural sources, the GAG's hydrophilic nature and lack of a suitable chromophore, and the GAG's acidity, fragility, polydispersity and heterogeneous sulfation make their characterization not readily amenable by NMR, reverse-phase HPLC and mass spectrometry,[6] respectively.

Here, we demonstrate that quartz crystal microbalance with dissipation monitoring (QCM-D), a surface-sensitive technique popular for biosensing applications, enables quantitative analysis of conjugation yields and stability with a few micrograms of GAGs of arbitrary complexity. To this end, we compared the biotinylation of GAGs via two different chemoselective ligation chemistries (Scheme 1A).[7] Hydrazone ligation has become the most frequently used strategy for GAG functionalization.[1, 8-10, 11] Oxime ligation (for selected references, see [12]), on the other hand, has only rarely been applied to polysaccharides,[13] and to our knowledge not to GAGs. We show that conventional hydrazone ligation is inefficient, in particular for long GAGs, due to a low yield, and confirm that hydrazone conjugates are unstable in aqueous environment.[14, 15] In contrast, oxime ligation emerges as a facile, rapid and efficient method that provides conjugates with higher stability and can be broadly applied, i.e. for different GAG types and for oligosaccharides as well as polymeric GAGs of high molecular weight.

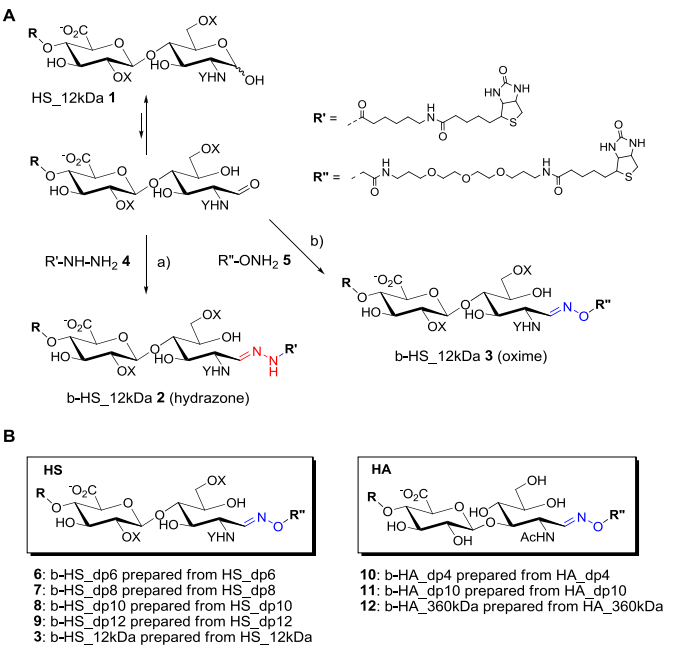

Scheme 1. (A) Strategies adopted for the biotinylation of GAGs at their reducing end, exemplified with a selected HS. Conditions: (a) **1** (0.33 mM), **4** (10 mM), PBS, pH 7.4, RT, 48 h; (b) **1** (4 mM), **5** (3.4 mM), aniline (100 mM), acetate buffer (100 mM), pH 4.5, 37°C, 48 h. (B) Library of biotin conjugates of the GAGs HS and HA of various size, prepared using oxime ligation. HS consists of GlcA β(1→4) GlcNAc α(1→4) disaccharides; X can be either H or SO_3H; Y can be either Ac or SO_3H. HA is unsulfated and consists of GlcA β(1→3) GlcNAc β(1→4) disaccharides. R = remaining GAG chain.

The reducing terminus of GAGs can selectively react with biotin derivatives presenting aminooxy or hydrazide groups to provide oxime and hydrazone linkage, respectively. For oxime ligation, the

reaction was successful only by using aniline as a catalyst as described previously.[16] To reproduce a commonly reported protocol,[1, 8, 10, 11] we did not use aniline for hydrazone ligation, although this compound is known to enhance also this reaction.[17] We created a library of biotin-conjugates through oxime ligation, containing GAGs of different type and defined chain length (Scheme 1B): hyaluronic acid (HA; oligosaccharides with 2 and 5 disaccharide units (dp4, dp10), and a 360 kDa polysaccharide) and heparan sulfate (HS; dp6, dp8, dp10, dp12, and a 12 kDa polysaccharide).

For b-HA_dp4 **10**, mass analysis (Fig. S1) demonstrated that one biotin molecule is attached per HA while NMR analysis (Fig. S2) confirmed that the biotin is attached at the reducing end, forming E and Z oxime isomers in a 73/27 ratio. Notably, these conventional characterization methods did not provide useful information for any of the other compounds produced.

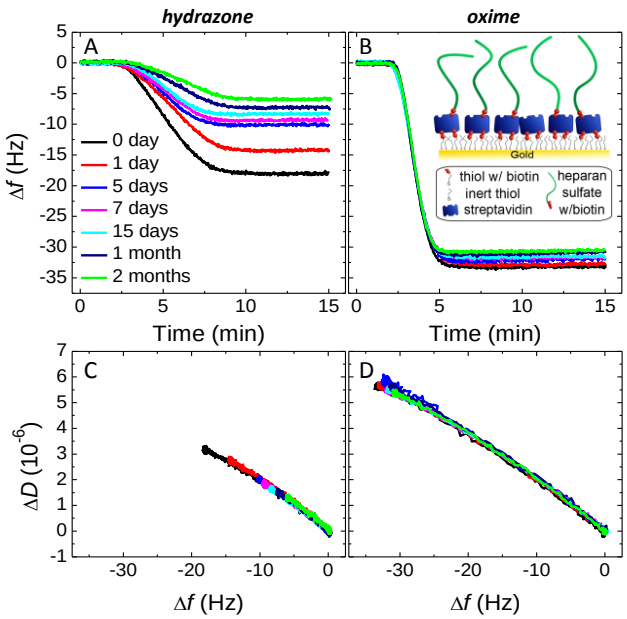

Figure 1. Binding assay to study the yield and stability of hydrazone and oxime conjugation. (A-B) QCM-D frequency shifts, Δ*f*, obtained for the specific binding of **2** (A) and **3** (B), stored at 4°C for variable times (as indicated), on streptavidin-coated surfaces (schematically shown in the inset). Samples were incubated for 10 min (from 2 to 12 min) at a total GAG concentration of 50 µg/mL, which was followed by exposure to buffer solution. (C-D) Parametric plots of QCM-D dissipation shifts, Δ*D* (not previously shown) vs. Δ*f* (from A and B, respectively). The plots inform about the evolution of the HS film mechanical properties and morphology with increasing surface coverage. All curves had comparable shapes, indicating that all compounds tested generate comparable film morphologies at a given surface coverage.

To characterize the conjugation of more complex GAGs, we exploited the high affinity of the streptavidin (SAv)-biotin interaction,[8, 18] and followed the binding of GAGs to surfaces displaying a SAv monolayer (Fig. 1B, inset) by QCM-D (Fig. S3). Figure 1A-B illustrates the differences in the stability of biotinylated HS (b-HS made from **1**, ~22 disaccharides) prepared through hydrazone and oxime ligation, **2** and **3**, respectively, as a function of storage time (up to two months) at 4 °C. The binding of b-HS samples was evaluated by two different parameters: the QCM-D frequency shift at saturation (Δf_{sat}; proportional to the areal mass density of immobilized b-HS (Fig. S4)) and the maximal binding rate ($\Delta f/\Delta t$; proportional to the concentration of b-HS in the sample solution (Fig. S5A)). The magnitudes of Δf_{sat} and $\Delta f/\Delta t$ decreased appreciably with increasing storage time for b-HS hydrazone (Fig. 1A), whereas only minor changes were observed for b-HS oxime (Fig. 1B). Moreover, the magnitudes of Δf and $\Delta f/\Delta t$ for **2** were lower than for **3**, even when de-frozen aliquots were used immediately. We argue that these effects are the result of the release of biotin upon degradation of the conjugates, i.e. the hydrazone but not the oxime is already appreciably degraded immediately after purification, and further degrades upon storage at 4 °C.

To understand this, we note that the QCM-D responses in Fig. 1 are exclusively due to binding of intact b-HS. Biotin-free HS did not bind (Fig. S3) and free biotin (produced as the result of degradation) did not by itself give rise to a measurable signal (Fig. S6). A decrease in the magnitude of Δf_{sat}, therefore, is consistent with partial occupancy of the surface with b-HS and saturation of the remaining binding sites by free biotin (Fig. S7). Further analysis of the QCM-D responses, including the dissipation shift Δ*D*, in terms of so-called Δ*D* vs. Δ*f* curves (Fig. 1C-D) revealed invariant curve shapes, indicating that the film morphology (at a given surface coverage) was comparable for all compounds tested. A plausible explanation is that the composition of the film in terms of the HS molecular conformation or size distribution is not altered by the degradation or the type of conjugation. This implies that degradation of b-HS occurs exclusively through cleavage of the bond that links biotin to HS, which is due to the hydrolysis of hydrazone (and to a much lesser extent oxime) under physiological conditions.[14]

We note in passing that the biotin released upon degradation would occupy a fraction of the available binding site on any biotin-capturing surface. This influences the surface density of immobilized GAGs, and thus entails a limited reproducibility of surface functionalization. This shortcoming needs to be considered, for example, in solid-phase molecular binding assays such as by surface plasmon resonance.[11, 19]

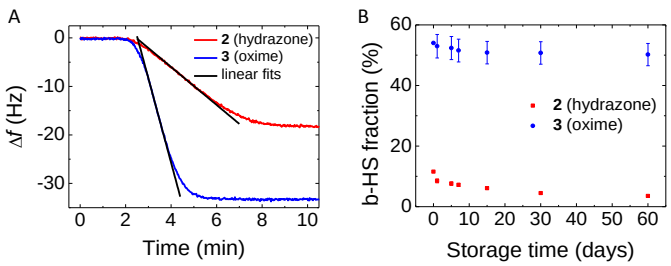

Figure 2. (A) Quantification of active analyte concentrations from QCM-D binding assays. The ratio of the slopes of the extended linear binding regimes (black lines are linear fits), here shown by way of example for freshly de-frozen b-HS hydrazone **2** (red line) and b-HS oxime **3** (blue line) (data from Fig. 1), is proportional to the ratio of the analytes' active concentrations. (B) Fraction of intact b-HS as a function of storage time at 4°C for **2** (red squares) and **3** (blue circles), determined through comparison of binding rates (data from Fig. 1). Error bars represent variations in the slopes observed for three independent measurements under identical conditions. Freshly de-frozen b-HS oxime **3**, for which the active analyte concentration was determined independently (Fig. S5), was used as a reference.

For a quantitative analysis of reaction yields and degradation rates, we determined steady-state binding rates (Figs. 2A and S5A) through linear fits to appropriate portions of the binding curves in Fig. 1A-B. At steady state, binding is mass-transfer limited, and with total HS concentrations and flow conditions maintained unchanged in our assay, any decrease in the binding rate reflects a proportional decrease in the concentration of intact b-HS in the probed solution (Figs. 2A and S5A).[20] From the binding rate of freshly de-frozen **3** and through comparison with a reference molecule of known concentration we could estimate the reaction yield of oxime ligation (Fig. S5); comparison of the binding rates in Fig. 1 then yielded the fraction of intact b-HS in all probed solutions (Fig. 2). The fraction

of biotinylated analyte in the freshly de-frozen **3** was 54 ± 8%. This value was confirmed by weighing **10** (which in contrast to larger GAGs could be readily separated from non-biotinylated GAGs; Fig. S1). The activity of freshly defrozen **2** was almost 5-fold smaller than that of **3**, indicating that reaction yields are considerably improved for oxime ligation (Fig. 2B). The 5-fold improvement in yield was confirmed by dot-blot analysis (Fig. S8). Moreover, the fraction of intact **2** decreased by another 5-fold over 60 days of storage at 4°C, indicating substantial degradation, whereas **3** was only marginally degraded over the same time interval (Fig. 2B).

Concerning the GAGs of various chain length, a clear trend in the Δ*f* values at saturation (Figs. 3A for HS and 3B-C for HA) and in the Δ*D* vs. Δ*f* curves (Fig. 3D-F) as a function of size confirmed that QCM-D curves are indeed sensitive to variations in molecular weight. Differences in molecular weight, as small as one disaccharide for oligomeric GAGs, can be readily distinguished through Δ*D* vs. Δ*f* curves (Fig. 3D, inset). Thus, the Δ*D* vs. Δ*f* curves represent a useful tool that provides insight into sample composition. HA_dp10 **8** bound to SAv monolayers with a response similar although not identical to HS_dp10 **11** (Figs. 3B and E). We propose that the slightly stronger Δ*f* shift for **8** over **11** reflects an increased film thickness, resulting from a stronger repulsion between the sulfated and thus more highly charged HS chains in **8**. Notably, even the long HA polymer **12** with ~900 disaccharides could be readily biotinylated (Fig. 3C), indicating that the polymer length does not affect conjugation.

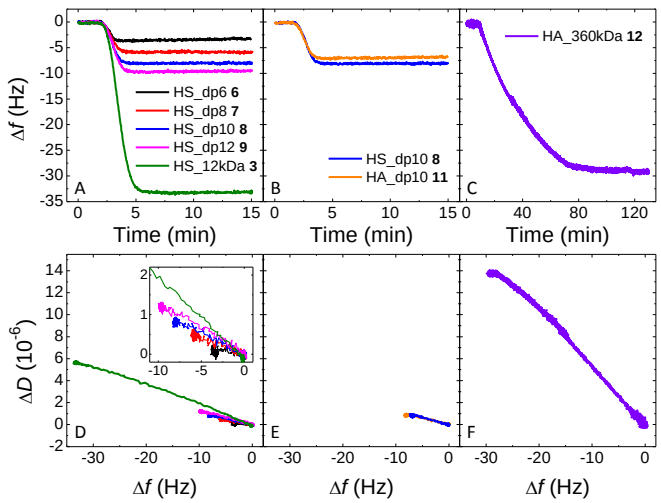

Figure 3. QCM-D binding assays for HS (A) and HA (B-C) of various sizes (as indicated). All GAGs were conjugated with biotin *via* oxime ligation. Data for **8** is also shown in B to facilitate comparison with **11**. Incubation conditions were as described in Fig. 1, except for **12**, which was incubated from 5 to 110 min. (D-F) Δ*D* vs. Δ*f* curves corresponding to A-C, respectively; the inset in D shows a part of the data at higher magnification. The magnitude of the slope of the Δ*D* vs. Δ*f* curves increases as a function of GAG size, indicating that larger GAGs generate a softer film.[21]

In summary, QCM-D together with a suitably functionalized sensor surface has proven instrumental for the characterization of conjugates made from chemically complex molecules such as GAGs, providing information about reaction yields, sample degradation and sample composition that is difficult to assess with conventional analytical techniques, in particular when the amount of sample is limited to a few micrograms. Moreover, we have established oxime ligation as a facile, one-step method for the selective conjugation of GAGs at the reducing end. The method is superior in yield and stability to the commonly used hydrazone ligation, and versatile in that it can be applied to GAGs of various (most likely any) types and sizes. The methods should find broad use, as tools in the glycosciences and in biotechnological applications. In particular, the control over and stability of GAG conjugates is crucial towards the reliable preparation of GAG-functionalized surfaces and scaffolds for tissue engineering and fundamental biological studies.[22]

We thank C. Travelet (Cermav, Grenoble, France) and G. Dubacheva (CIC biomaGUNE) for support with DLS and SE measurements, respectively, E. Defrancq and N. Spinelli (DCM) for oligonucleotide synthesis and R. Vivés (IBS) for preparation of HS oligomers. This work was supported by the Nanosciences Foundation (Grenoble) through the Chair of Excellence Project GAG2D (to R.P.R.) and a PhD scholarship (to D.T.), the NanoBio programme, the ICMG FR 2607 and the LabEx ARCANE (ANR-11-LABX-0003-01).

Notes and references

[a] Université Grenoble Alpes, DCM, 38000 Grenoble, France
[b] CNRS, DCM, 38000 Grenoble, France
[c] Université Grenoble Alpes, Institut de Biologie Structurale (IBS), 38027 Grenoble, France
[d] CNRS, IBS, 38027 Grenoble, France
[e] CEA, DSV, IBS, 38027 Grenoble, France
[f] CIC biomaGUNE, Paseo Miramon 182, 20009 Donostia - San Sebastian, Spain. E-mail: rrichter@cicbiomagune.es; Tel: +34 943 00 53 29
[g] Max Planck Institute for Intelligent Systems, 70569 Stuttgart, Germany

Electronic Supplementary Information (ESI) available: Supplementary materials and methods, synthesis of a precursor, supplementary figures and references. See DOI: 10.1039/c000000x/

1. E. Mercey, R. Sadir, E. Maillart, A. Roget, F. Baleux, H. Lortat-Jacob and T. Livache, *Anal. Chem.*, 2008, **80**, 3476-3482.
2. W. Takada, M. Fukushima, P. Pothacharoen, P. Kongtawelert and K. Sugahara, *Anal. Biochem.*, 2013, **435**, 123-130; E. Clo, O. Blixt and K. J. Jensen, *Eur. J. Org. Chem.*, 2010, 540-554; S. Park, J. C. Gildersleeve, O. Blixt and I. Shin, *Chem. Soc. Rev.*, 2013, **42**, 4310-4326.
3. M. Morra, *Biomacromolecules*, 2005, **6**, 1205-1223.
4. J. A. Burdick and G. D. Prestwich, *Adv. Mater.*, 2011, **23**, H41-56.
5. N. Altgarde, J. Becher, S. Moller, F. E. Weber, M. Schnabelrauch and S. Svedhem, *J. Colloid Interface Sci.*, 2013, **390**, 258-266.
6. Zaia, *Biomacromol. Mass Spectrom.*, 2005, **1**, 3-36.
7. J. A. Prescher and C. R. Bertozzi, *Nat. Chem. Biol.*, 2005, **1**, 13-21.
8. N. Altgarde, E. Nileback, L. de Battice, I. Pashkuleva, R. L. Reis, J. Becher, S. Moller, M. Schnabelrauch and S. Svedhem, *Acta Biomater.*, 2013, **9**, 8158-8166.
9. K. Godula and C. R. Bertozzi, *J. Am. Chem. Soc.*, 2010, **132**, 9963-9965.
10. H. Ichijo, N. Sugiura and K. Kimata, *Polymers*, 2013, **5**, 254-268; T. Mori, T. Kodera, H. Yoshimine, Y. Kakuta, N. Sugiura, K. Kimata and Y. Okahata, *Chemistry*, 2012, **18**, 7388-7393.
11. E. Saesen, S. Sarrazin, C. Laguri, R. Sadir, D. Maurin, A. Thomas, A. Imberty and H. Lortat-Jacob, *J. Am. Chem. Soc.*, 2013, **135**, 9384-9390.
12. F. Peri, P. Dumy and M. Mutter, *Tetrahedron*, 1998, **54**, 12269-12278; R. D. Goff and J. S. Thorson, *Med. Chem. Commun.*, 2014, in press; F. Lin, J. Zheng, J. Yu, J. Zhou and M. L. Becker, *Biomacromolecules*, 2013, **14**, 2857-2865.

13. T. J. Styslinger, N. Zhang, V. S. Bhatt, N. Pettit, A. F. Palmer and P. G. Wang, *J. Am. Chem. Soc.*, 2012, **134**, 7507-7515; A. Richard, A. Barras, A. B. Younes, N. Monfilliette-Dupont and P. Melnyk, *Bioconjugate Chem.*, 2008, **19**, 1491-1495; T. T. Beaudette, J. A. Cohen, E. M. Bachelder, K. E. Broaders, J. L. Cohen, E. G. Engleman and J. M. J. Frechet, *J. Am. Chem. Soc.*, 2009, **131**, 10360-10361.
14. J. Kalia and R. T. Raines, *Angew. Chem., Int. Ed.*, 2008, **47**, 7523-7526.
15. A. A. Kale and V. P. Torchilin, *Bioconjugate Chem.*, 2007, **18**, 363-370; B. Levrand, Y. Ruff, J.-M. Lehn and A. Herrmann, *Chem. Commun.*, 2006, 2965–2967.
16. M. B. Thygesen, H. Munch, J. Sauer, E. Clo, M. R. Jorgensen, O. Hindsgaul and K. J. Jensen, *J. Org. Chem.*, 2010, **75**, 1752-1755.
17. J. Y. Byeon, F. T. Limpoco and R. C. Bailey, *Langmuir*, 2010, **26**, 15430-15435.
18. N. S. Baranova, E. Nileback, F. M. Haller, D. C. Briggs, S. Svedhem, A. J. Day and R. P. Richter, *J. Biol. Chem.*, 2011, **286**, 25675-25686.
19. R. I. W. Osmond, W. C. Kett, S. E. Skett and D. R. Coombe, *Anal. Biochem.*, 2002, **310**, 199-207.
20. W. T. Hermens, M. Benes, R. Richter and H. Speijer, *Biotechnol. Appl. Biochem.*, 2004, **39**, 277-284.
21. I. Reviakine, D. Johannsmann and R. P. Richter, *Anal. Chem.*, 2011, **83**, 8838-8848.
22. E. Migliorini, D. Thakar, R. Sadir, T. Pleiner, F. Baleux, H. Lortat-Jacob, L. Coche-Guerente and R. P. Richter, *Biomaterials*, 2014, **35**, 8903-8915.

